Plasmonic enhancement of single-molecule fluorescence under one- and two-photon excitation

Lu, X.

2

Theoretical investigations of the single-molecule fluorescence enhancements by a single gold nanorod and by an end-to-end gold nanorod dimer

Single gold nanorod supports the longitudinal plasmon modes that may enhance not only the near-fields but also the local density of photon states near the tips. As a consequence, single gold nanorods can be used to enhance the fluorescence of weak emitters, by enhancing both the excitation and radiative rates. Gold nanorod dimer, arranged in an end-to-end configuration, may strengthen both effects inside the gap owing to the strong plasmon coupling. This provides stronger fluorescence enhancement. We compare the fluorescence enhancement by a single gold nanorod to that of a gold nanorod dimer with interparticle gap of $5\,\mathrm{nm}$*. We consider fluorescent dyes with different absorption and emission bands. Our simulations reveal that, at weak excitation, an enhancement factor of* $\sim 10^4$ *can be achieved by the dimer for one-photon excited fluorescence, while for two-photon-excited fluorescence, the enhancement factor by the dimer can be as high as* $\sim 10^8$*. The influence of plasmon modes on the fluorescence lifetime and on the spectral shaping is also investigated for all the dyes. At high excitation intensity, the enhancement factor for both one- or two-photon-excited fluorescence will be saturated to a limited value of the radiative enhancement by the plasmonic structures.*

2.1. Introduction

The most valuable feature of noble metal nanoparticles comes from the collective oscillation of surface charges, also known as the localized surface plasmon resonance (SPR)[1, 2]. Controlling the SPR of nanoparticles provides an effective way of manipulating the light-matter interaction on the nanoscale[3–6]. As a straightforward approach, coupling to plasmonic nanoparticles can strongly influence the fluorescence processes of fluorophores[7–19]. First of all, the excitation efficiencies of the fluorophores can be largely enhanced due to the strong light-field confinement near the plasmonic nanoparticles. Secondly, the SPR of the nanoparticles may also increase the local density of photon states (LDOS) around the surfaces, which, in turn, enhances the radiative rate of the excited fluorophore according to the Purcell effect[20, 21]. The emission rates of the emitters, however, may be quenched via the additional non-radiative channels induced by the Ohmic absorption of the metal[8, 22, 23]. Consequently, the interplay of these effects may result in an overall enhancement of the fluorescence rates, and can modify the fluorescence lifetimes[23–25] and the spectral shapes of emissions[26–29], which can be controlled by tuning the shapes and sizes of the metal nanoparticles, as well as the relative position and orientation of the emitter with respect to the nanoparticles[11].

The impacts of plasmon resonance on the emission properties of a single fluorophore can be theoretically investigated by solving the classical Maxwell's equations, involving a radiative dipole coupled to the plasmonic structure[10, 13, 17–19]. In this chapter, we evaluate theoretically the performance of gold nanorod based SPR on the fluorescence enhancement of very weak emitters, which are harder to detect at single-molecule level, either because of the very small quantum yields, or because of the very low excitation efficiencies in certain cases, for example two-photon excitation[30]. In the following sections, we will examine the fluorescence enhancement by a single GNR and compare it with the enhancement by a GNR dimer structure, where the GNRs couple strongly with each other. Moreover, we will also investigate the influences of the LSPRs of these plasmonic nanostructures on the fluorescence lifetime and on the shape of the emission spectra. At last, we will investigate the saturation of the fluorescence of a molecule at high excitation, with or without the enhancement by the plasmonic structures.

2.2. Theoretical framework

Two-level scheme of fluorescence enhancement by an antenna

In this thesis, we follow the two-level scheme of Khatua et al[13]. to study the single-molecule fluorescence enhancement by a plasmonic nanoantenna. In this model, the fast internal vibration relaxation is ignored, and the transition rates of the molecule between the ground (g) and exited (e) state are represented by the excitation and the two relaxation rates, as depicted in figure 1. In the absence of the nano-antenna, the time evolution of the probabilities of the molecule at the excited state (p_{e}^{0}) and at the ground state (p_{g}^{0}) can be

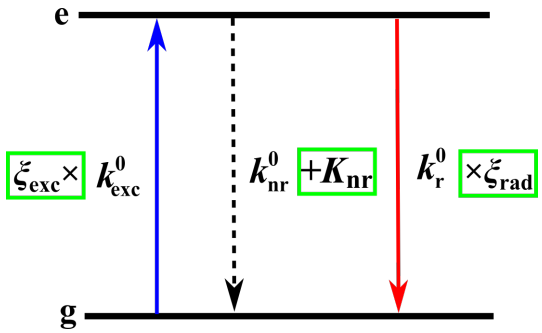

Figure 2.1: Schematic of the transition rates of a molecule in a two-level system, with or without a nanoantenna. Reprinted from Ref[13].

expressed as

$$\begin{aligned} \frac{\mathrm{d}p^0_\mathrm{e}}{\mathrm{d}t} &= k^0_\mathrm{exc} \cdot p^0_\mathrm{g} - (k^0_\mathrm{nr} + k^0_\mathrm{r}) p^0_\mathrm{e} \\ p^0_\mathrm{g} &= 1 - p^0_\mathrm{e}, \end{aligned} \tag{2.1}$$

which, at the steady state condition of $\frac{\mathrm{d}p^0_\mathrm{e}}{\mathrm{d}t} = 0$, gives the equilibrium population of the excited state,

$$p^0_\mathrm{e} = \frac{k^0_\mathrm{exc}}{k^0_\mathrm{exc} + k^0_\mathrm{nr} + k^0_\mathrm{r}}. \tag{2.2}$$

The photon emission rate from the molecule is given by

$$I^0_\mathrm{f} = \frac{k^0_\mathrm{exc} \cdot k^0_\mathrm{r}}{k^0_\mathrm{exc} + k^0_\mathrm{nr} + k^0_\mathrm{r}} = k^0_\mathrm{exc} \cdot \frac{1}{k^0_\mathrm{exc}/k^0_\mathrm{r} + 1/\eta_0}. \tag{2.3}$$

Here, k^0_r and k^0_nr are the radiative and non-radiative rates of the molecule, k^0_exc is the excitation rate, and η_0 represents the quantum yield of the molecule. At low excitation power, where $k^0_\mathrm{exc}/k^0_\mathrm{r} \ll 1/\eta_0$, the emission rate is proportional to the excitation rate: $I^0_\mathrm{f} = k^0_\mathrm{exc} \cdot \eta_0$.

By replacing the transition rates in equation (2.3) with the rates modified by the antenna, we get the enhanced emission rate in the presence of the antenna

$$I_\mathrm{f} = \xi_\mathrm{exc} \cdot k^0_\mathrm{exc} \cdot \frac{\xi_\mathrm{rad}}{\xi_\mathrm{exc} \cdot k^0_\mathrm{exc}/k^0_\mathrm{r} + (\xi_\mathrm{rad} + K_\mathrm{nr}/k^0_\mathrm{r} - 1) + 1/\eta_0}, \tag{2.4}$$

and the overall fluorescence enhancement by the antenna

$$\xi_\mathrm{total} = \xi_\mathrm{exc} \cdot \xi_\mathrm{rad} \cdot \frac{k^0_\mathrm{exc}/k^0_\mathrm{r} + 1/\eta_0}{\xi_\mathrm{exc} \cdot k^0_\mathrm{exc}/k^0_\mathrm{r} + (\xi_\mathrm{rad} + K_\mathrm{nr}/k^0_\mathrm{r} - 1) + 1/\eta_0}. \tag{2.5}$$

Here ξ_exc and ξ_rad are the enhancement factors of the excitation and radiative decay rates, respectively. K_nr is the additional non-radiative absorption rate due to the dissipative losses

of the antenna. Under weak excitation the overall enhancement can be simplified as

$$\xi_{\mathrm{total}} = \xi_{\mathrm{exc}} \cdot \xi_{\mathrm{rad}} \cdot \frac{1/\eta_0}{(\xi_{\mathrm{rad}} + K_{\mathrm{nr}}/k_{\mathrm{r}}^0 - 1) + 1/\eta_0}. \tag{2.6}$$

As a result of the modification of the decay rates by the antenna, the fluorescence of the molecule can be deduced as

$$\frac{\tau}{\tau_0} = \frac{k_{\mathrm{r}}^0 + k_{\mathrm{nr}}^0}{\xi_{\mathrm{rad}} k_{\mathrm{r}}^0 + k_{\mathrm{nr}}^0 + K_{\mathrm{nr}}} = \frac{1/\eta_0}{(\xi_{\mathrm{rad}} + K_{\mathrm{nr}}/k_{\mathrm{nr}}^0 - 1) + 1/\eta_0}. \tag{2.7}$$

Here, for simplicity, we omit the intersystem transitions of the excited molecule to other energy states, which may cause fluorescence blinking, or phosphorescence of the molecules.

Numerical simulations of fluorescence enhancements

The fluorescence enhancement of a single molecule by the plasmonic antenna can be treated classically, provided the molecule is not too close to the metal (sub-nanometer away from the metal surfaces). We consider the molecule as a radiative dipole $\mathbf{p}_0$ oscillating with frequency of ω. As the theoretical absorption rate of the molecule is related to the intensity of the local field at its position, the excitation enhancement factor by the nanoantenna can be expressed as

$$\xi_{\mathrm{exc}}^{(n)} = \frac{|\mathbf{p}_0 \cdot \mathbf{E}(\omega_{\mathrm{exc}})|^{2n}}{|\mathbf{p}_0 \cdot \mathbf{E}_0(\omega_{\mathrm{exc}})|^{2n}}, \tag{2.8}$$

where $\mathbf{E}(\omega_{\mathrm{exc}})$ and $\mathbf{E}_0(\omega_{\mathrm{exc}})$ are the electric fields at the position of the dipole with and without the nanoantenna, ω_{exc} is the frequency of the illuminating light source, and the number $n = 1\ or\ 2$ indicates the excitation with one or two photons, since two-photon absorption depends on the square of the excitation light intensity[31, 32].

To evaluate the enhancement factor by the nanoantenna numerically, we applied a classical electrodynamics approach based on boundary element method (SCUFF-EM) to simulate the excitation and emission enhancements[33, 34].

To get the excitation enhancement, we assumed the antenna is excited by a plane wave and for the calculation of decay rates, we modeled the excited emitter as a radiating dipole, whose time-averaged radiated power in a medium without nanoantenna is[4]

$$P_{r0}(\omega) = \frac{|\mathbf{p}_0|^2}{4\pi\varepsilon_0} \frac{n\omega^4}{3c^3}, \tag{2.9}$$

where n is the refractive index of the medium, c is the speed of light and ε_0 is the vacuum permittivity. The enhancement factor of the radiative rate (ξ_{rad}) and the non-radiative dissipation rate (K_{nr}) by the nanoantenna were derived from

$$\xi_{\mathrm{rad}} = k_{\mathrm{r}}/k_{\mathrm{r}}^0 = P_{\mathrm{rad}}/P_{\mathrm{r0}}, \tag{2.10}$$

and

$$K_{\mathrm{nr}}/k_{\mathrm{r}}^0 = P_{\mathrm{abs}}/P_{\mathrm{r0}}. \tag{2.11}$$

In the simulations, the power absorbed by the antenna P_{abs} was calculated by integrating the Poynting vector over the surface, and the radiated power P_{rad} was obtained from[4]

$$P_{\mathrm{rad}}(\omega) + P_{\mathrm{abs}}(\omega) = \frac{\omega^3}{2c^2\varepsilon_0}|\mathbf{p}_0|^2[\mathbf{n} \cdot \mathrm{Im}[\mathbf{G}(\mathbf{r}, \mathbf{r}; \omega)] \cdot \mathbf{n}], \tag{2.12}$$

where $\mathbf{G}(\mathbf{r}, \mathbf{r}; \omega)$ is the Green tensor at the emitter's position $\mathbf{r}$ and $\mathbf{n}$ represents the direction of the dipole moment.

From Eqs. (S3.12) and (S3.15), we can clearly see that the radiative rate enhancement ($\xi^{\omega}_{\mathrm{rad}}$) and the non-radiative relaxation rate $K^{\omega}_{\mathrm{nr}}(\omega)$ both depend on the frequency of the emitted photons (ω). To get the emission enhancement for all the photons, we calculate the average radiative rate enhancement and non-radiative relaxation rate:

$$<\xi_{\mathrm{rad}}>= \int \xi_{\mathrm{rad}}(\omega)F_{\mathrm{dye}}(\omega)d\omega, \tag{2.13}$$

$$<K_{\mathrm{nr}}>= \int K_{\mathrm{nr}}(\omega)F_{\mathrm{dye}}(\omega)d\omega, \tag{2.14}$$

here, $F_{\mathrm{dye}}(\omega)$ is the normalized emission spectra of the molecule.

2.3. Results and discussion

The most valuable feature of gold nanorod (GNR) dimers compared to single GNR, comes from their outstanding capacity of enhancing ultra-weak signals[35–38]. As an example, we first compare the fluorescence enhancement by an end-to-end GNR dimer with the enhancement by a single GNR.

We start from the strongest coupled dimer configuration, where two identical GNRs are arranged in end-to-end manner with the long axes along each other, shown in figure 2.3a. All GNRs were modeled as a cylinder with two hemispheres at the ends, and their diameters were fixed at a constant value of $40\ \mathrm{nm}$. For the single GNR, the length was set as $115\ \mathrm{nm}$, which gives a longitudinal plasmon resonance of $765\ \mathrm{nm}$. While for the GNR dimer, we adjust the length and the interparticle gap to tune the resonance of the longitudinal-coupled mode to the same plasmon wavelength as the single GNR. In order to have enough space for the molecule to access the near-field hotspot, the GNRs were separated by a gap of $5\ \mathrm{nm}$, and their lengths were adjusted to $90\ \mathrm{nm}$, which ensures the longitudinal plasmon resonance at the wavelength of $765\ \mathrm{nm}$. In the simulations, the dielectric constant for gold was taken from Johnson and Christy, and the refractive index of the ambient medium was taken as 1.33 for water.

For simplicity, the fluorescent molecule was modeled as a point dipole with orientation to be parallel to the polarization of the excitation light, which was aligned with the long axis to get the best excitation. For the single GNR, we placed the molecule at varied positions along the long axis with a certain distance (labeled as 'd' in figure 2.2a) from the tip of the GNR. For the GNR dimer, the position of the molecule is represented by the distance d from the tip of the first GNR (as shown in figure 2.3a) between the two GNRs along the long axes. For both cases, the minimum distance of the molecule away from the gold surface was assumed to be $0.75\ \mathrm{nm}$.

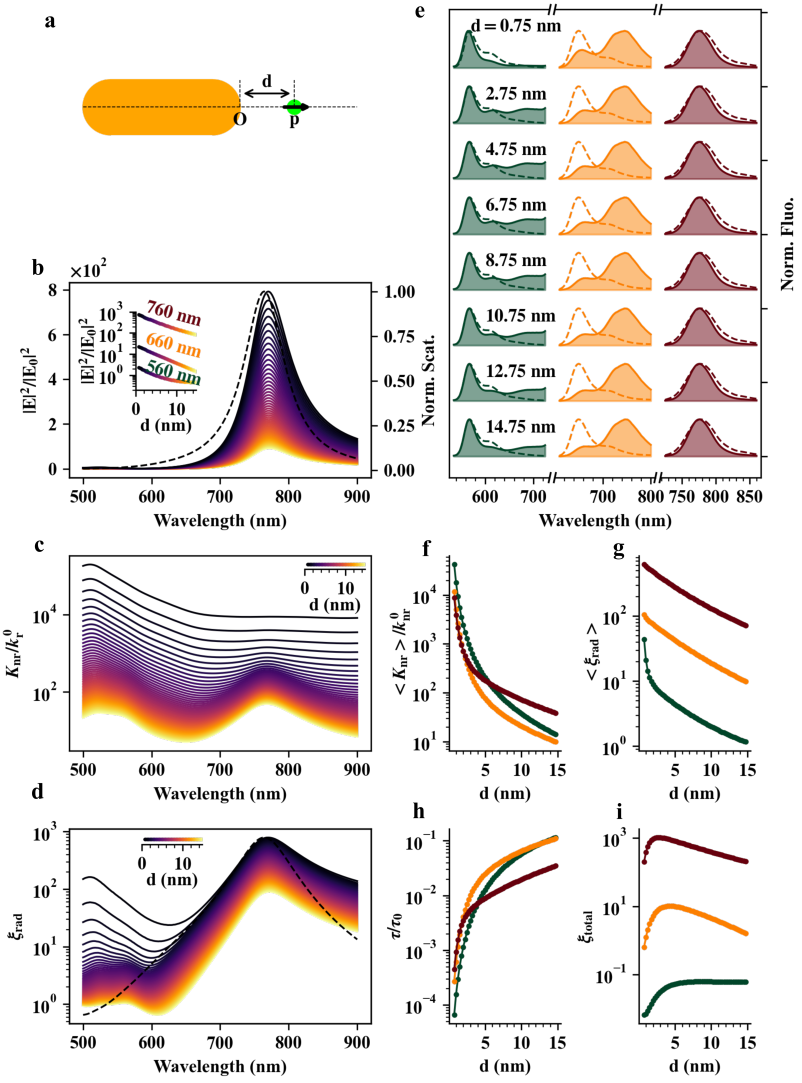

Figure 2.2: Calculated fluorescence enhancement by a single GNR. (a) Scheme of the simulation. (b) Near-field intensity enhancements as a function of the excitation wavelength at different distances. The distance is represented by the color of the line, which corresponds to the d-ordinate of the dots of the same color in the inset. Black dashed line is the normalized scattering spectrum of the GNR. Inset shows the near-field intensity enhancements as a function of d excited at the wavelengths of 760 nm, 660 nm and 560 nm. (c, d) Additional non-radiative rates (c) and radiative enhancements (d) as a function of wavelength at different distances. Dashed line in (d) is the normalized scattering of GNR. (e) Spectral shaping of the spontaneous emissions from three dyes with different emission bands near a single GNR with different separations (labeled by the values of d). Left to right: the original (dashed line) and modified (shaded) emission spectra of Alexa Fluor 555 (dark green), Alexa Fluor 633 (orange) and Alexa Fluor 750 (brown). (f-i) Distance dependence of the averaged additional non-radiative rate (f), radiative enhancement (g), lifetime shortening (h) and overall enhancement (i) for the molecules of Alexa Fluor 555 (dark green), Alexa Fluor 633 (orange) and Alexa Fluor 750 (brown).

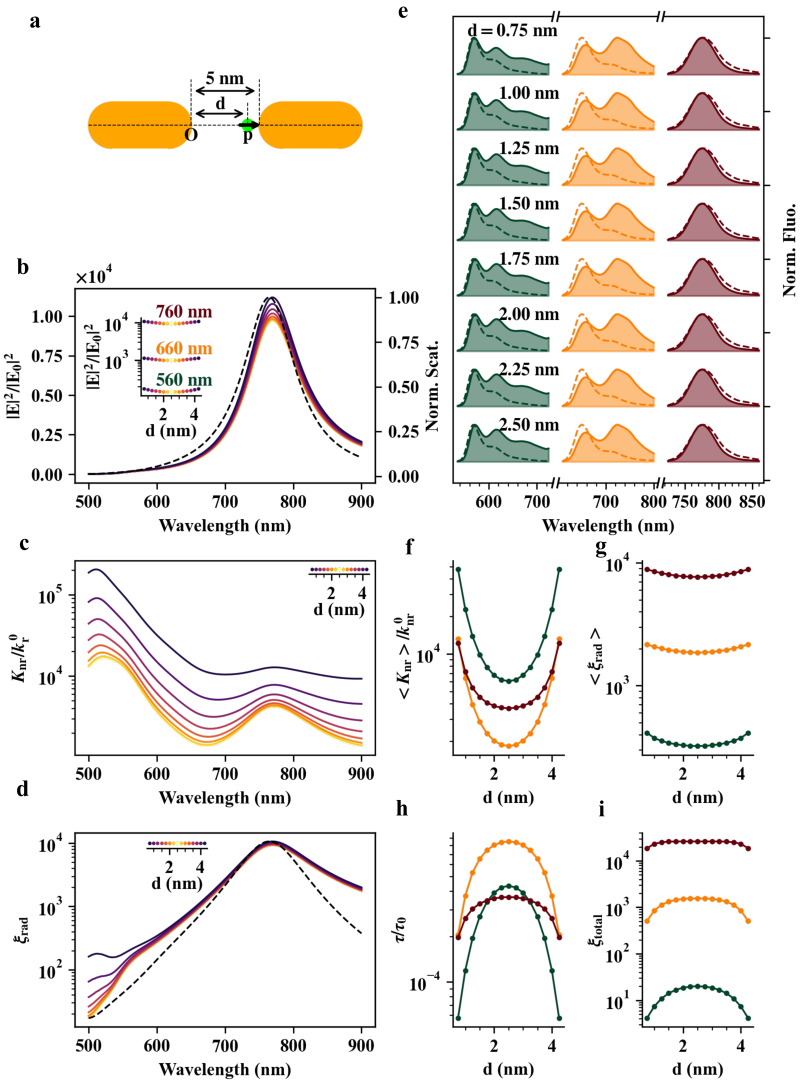

Figure 2.3: Calculated fluorescence enhancement by a GNR dimer. (a) Scheme of the simulation. (b) Near-field intensity enhancements as a function of the excitation wavelength at different positions represented by d, which corresponds to the d-ordinate of the dot in the inset with respect to the line-color. Black dashed line is the normalized scattering spectrum of the GNR dimer. Inset shows the near-field intensity enhancements as a function of d excited at the wavelengths of 760 nm, 660 nm and 560 nm. (c, d) Additional non-radiative rates (c) and radiative enhancements (d) as a function of wavelength at different positions. Dashed line in (d) is the normalized scattering of GNR dimer. (e) Spectral shaping of the spontaneous emissions from three dyes with different emission bands at different positions inside the gap of the GNR dimer (labeled by the values of d). Left to right: the modified (shaded) and original (dashed line) emission spectra of Alexa Fluor 555 (dark green), Alexa Fluor 633 (orange) and Alexa Fluor 750 (brown). (f-i) Position dependence of the averaged additional non-radiative rate (f), radiative enhancement (g), lifetime shortening (h) and overall enhancement (i) for the molecules of Alexa Fluor 555 (dark green), Alexa Fluor 633 (orange) and Alexa Fluor 750 (brown).

Enhancement of near-field intensity : Single GNR vs GNR dimer

Under weak excitation, the fluorescence enhancement can be treated as the product of the excitation enhancement and the emission enhancement. We first discuss the excitation enhancement upon one-photon absorption, which can be represented as the near-field intensity enhancement in the parallel-excited condition. Figure 2.3b shows the intensity enhancement of the near-field by the GNR dimer as a function of the excitation wavelength and of the molecular position (inset). For comparison, we also calculate the near-field intensity enhancement by a single GNR for different molecule-tip separations in figure 2.2b. From the plots, we can see that the intensity enhancement spectra of both structures are slightly red-shifted compared to the scattering spectra (from $765\ \mathrm{nm}$ to $770\ \mathrm{nm}$), and their shapes show clear asymmetric profiles, with the red wings decreasing slower than the blue wings as the excitation was detuned away from the resonant excitation. Such differences can be explained as the results of plasmonic damping and the dephasing between the near-field and the far-field responses of the structures.

Apparently, the near-field enhancement by a single GNR depends strongly on the position of the molecule with respect to the gold surface. As the molecule moves away from the tip of the GNR, the near-field enhancement decreases rapidly. Therefore, the effective excitation enhancement by a single GNR is only localized to a small volume near the tip. The GNR dimer provides a more uniform near-field hotspot with larger enhancement factor between the gap, which is distributed symmetrically along the long axis. From figure 2.2b, we can see the enhancement of near-field intensity by a single GNR in resonance drops monotonically from 7.9×10^2 to 3.6×10^2 as the GNR-molecule distance increases from $0.75\ \mathrm{nm}$ to $5\ \mathrm{nm}$. For the GNR dimer, however, the enhancement of the near-field intensity shows little change inside the gap. As shown in figure 2.3b, the enhancement factor decreases slightly from 1.0×10^4 to 0.9×10^4 as the molecule moves away from one tip at the distance of $0.75\ \mathrm{nm}$ toward the center of the dimer.

Additionally, GNR dimer performs better for the near-field enhancement excited at the wavelength out of the plasmon resonance. As an example, we compared the enhancement of the near-field intensity by the single GNR and by the GNR dimer at different excitation wavelengths as shown in the insets of figures 2.2a and 2.3a, respectively. We can see that the near-field intensity enhancement by the single GNR, for $d = 0.75\ \mathrm{nm}$, decreased from 730 to 23 and 2.3 as the excitation wavelength was detuned from $760\ \mathrm{nm}$ to $660\ \mathrm{nm}$ and $560\ \mathrm{nm}$, respectively. On the other hand, for the dimer the relative enhancement factor at these wavelengths drops from 1.1×10^4 to 1.1×10^3 and 1.7×10^2, respectively.

Non-radiative and radiative rates enhancement : Single GNR vs GNR dimer

Next, we examine the emission enhancement of the fluorescent molecule by the single GNR and by the GNR dimer. Unlike the excitation enhancement, where the near-field enhancement is due to the plasmon modes excited by a plane wave, the emission enhancement concerns the plasmon oscillation induced by a point-like dipole source, which may introduce different coupling channels to the plasmon modes. For instance, as the result of symmetry breaking, it may be easier for the dipole to excite the higher order modes or 'dark' modes of the plasmon structures compared to plane waves. As it was mentioned before, the influence of plasmon resonance on the emission properties of the dipole can be described by the enhancement of the radiative rates (ξ_{rad}) and the additional non-radiative rates ($K_{\mathrm{nr}}/k_{\mathrm{r}}^0$).

As shown in figures 2.2c and 2.3c, for both the single GNR and the GNR dimer, two major additional non-radiative absorption bands exist for the excited molecule. The first absorption band is due to the excitation of the longitudinal plasmon mode with the peak at wavelength of $770\ \mathrm{nm}$. The other one is at the high energy range with the peak at $510\ \mathrm{nm}$ which can be viewed as the result of the excitation of high-order modes. The excitation of the high-order modes and their coupling with far-field or other plasmonic modes, strongly depend on the excitation wavelength, the curvature of the gold surface and the distance of the dipole source from the surface. When the molecule is placed very close to the tip of the GNR (or close to the tip of one GNR in the case of the dimer), the additional dissipation channels are dominated by the high-order absorption modes. As the molecule moves away from the tip, the high-order absorption decreases more rapidly than the absorption due to the SPR, leaving two distinguishable peaks at wavelengths of $510\ \mathrm{nm}$ and $770\ \mathrm{nm}$ for both single GNR and GNR dimer.

To investigate the radiative rate enhancement, we need to consider not only the excitation of the plasmon modes by a dipole source, but also the coupling of these modes with the far fields. Different from the coupling with the point-like dipole source near by, low order plasmon modes with longer resonant wavelengths couple more efficiently with the far fields. This statement can be confirmed by the dominant peaks of the radiative enhancements at the wavelength of $770\ \mathrm{nm}$, as is shown in figures 2.2d and 2.3d, which correspond to the longitudinal plasmon resonances of singe GNR and GNR dimer, respectively. At this wavelength, due to the strong plasmon coupling between the GNRs, the radiative rate of the molecule inside the gap of the dimer can be enhanced by a factor of about 10^4, which is more than one order higher than the enhancement by a single GNR for the molecule separated by similar distance from the tip. From the spectra, we also see a small peak at $510\ \mathrm{nm}$ for both cases as the molecule is placed very close to the GNR's tip. This peak vanishes very quickly as we increase distance of the molecule from the GNR's tip. Additionally, for the radiative rate enhancement by the GNR dimer, we see more features in range between the two main modes compared to single GNR, which can be viewed intuitively as due to the excitation of other hybrid modes of the GNR dimer (except the longitudinal SPR) by the molecule.

Specifically, we notice that the high-order modes excited at the short wavelength of $510\ \mathrm{nm}$ are strongly localized modes. As a consequence, the excitation of this high-order modes is not influenced by the length of the GNR. From figure 2.4a, we can see that the additional non-radiative absorption at the wavelength of $510\ \mathrm{nm}$ by single GNR is not dependent on the length of the GNR. As the molecule moves away from the GNR's tip, the high-order absorption peaks by the single GNR decrease about two orders faster compared to the absorption at the SPRs of each GNR shown in figure 2.4b, indicating that the interaction length scale of the high order modes is about two-order smaller than the dipole-like longitudinal plasmon modes. From figure 2.4a, we also see that, for the GNR dimer, as the molecule inside the gap is placed very close to one of the two GNRs (e.g. $d \leq 1.5\ \mathrm{nm}$), the existence of the other GNR does not influence the values of additional non-radiative rates, which confirms the interaction length scales of these high order modes are absolutely short. Similar behaviour can be seen for the radiative rate enhancements for the single GNR and GNR dimer at the wavelength of $510\ \mathrm{nm}$, shown in figure 2.4c, where we don't see significant difference in the enhancement factors for all the structures, while the molecule is closer to GNR's tip. As a comparison, for radiative rate at SPR's wavelength, the enhancement

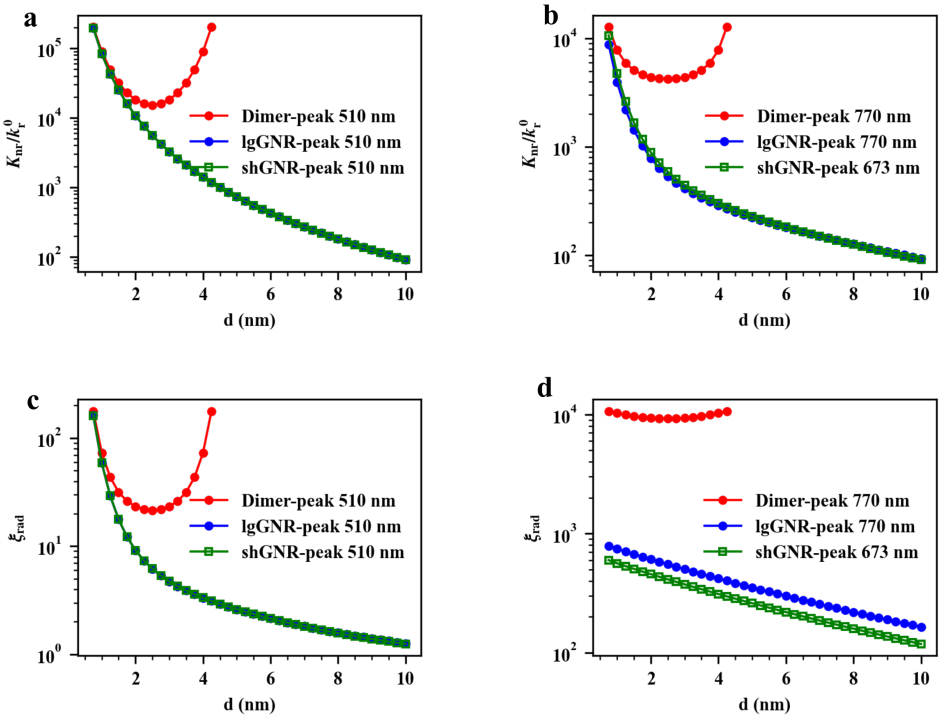

Figure 2.4: Comparisons of the additional non-radiative rates (a, b) and the radiative enhancements (c, d) at the wavelengths of 510 nm (a, c) and 770 nm (b, d), with the enhancements by a GNR dimer and by two single GNR of different lengths. The shorter single GNR (shGNR) with SPR of 670 nm has similar length as the individual GNR of the dimer, and the longer GNR (lgGNR) and the GNR dimer have same resonant wavelength of 765 nm.

factor by the GNR dimer can be more than one-order higher than the enhancement by a single GNR, as is shown in figure 2.4d.

Fluorescence enhancement of the dyes with different emission bands : Single GNR vs GNR dimer

So far, we have provided a detailed description of the influence of plasmon resonance on the excitation and radiation of a dipole emitter by exploiting a single GNR and a longitudinally arranged GNR dimer. To investigate the overall fluorescence enhancement of a dye molecule, we need to involve the influences of the intrinsic non-radiative decay of the molecule, and of the spectral overlaps of the molecular absorption and emission with the SPR. For a dye with specific absorption and emission bands, the well known strategy to get best fluorescence enhancement is to tune the plasmon resonance by adjusting its size to ensure best spectral overlaps between the SPR and the absorption and emission bands of the molecule.

Herein, we will compare the fluorescence enhancements by the aforementioned single GNR and GNR dimer for three dyes with very different absorption and emission bands: the Alexa Fluor 555, Alexa Fluor 633 and Alexa Fluor 750. They have similar quantum yield of 10% and different maximum absorption peaks at the wavelengths of $555\ \mathrm{nm}$, $633\ \mathrm{nm}$ and $750\ \mathrm{nm}$, respectively. Instead of tuning the plasmon resonances to get best fluorescence enhancements, we will use the same structures to investigate the enhancement of these three dyes under the excitation wavelengths of $560\ \mathrm{nm}$, 660 and $760\ \mathrm{nm}$, respectively. In the case of one-photon excitation, we lose both excitation and emission enhancement for the two dyes Alexa Fluor 555 and Alexa Fluor 633, which are off-resonance with the plasmonic structures. Yet the discussions about the spectral shaping and lifetime shortening by the GNR structures will be very valuable for the study of fluorescence enhancement under two-photon excitation, as the two-photon absorption bands for common dyes are normally in the infrared region and their excitation rates can be significantly enhanced by our structures, especially by the GNR dimers.

Spectral shaping of the spontaneous emission

One notable feature of the plasmon-emitter system is that the line-shape of the emission spectrum of the molecule can be modified, since different spectral components of the emission will be selectively enhanced according to the plasmonic modes. Here, we illustrate the modification of the emission spectra of the three dyes with very different emission bands by the single GNR and by the GNR dimer.

First, we have a look at the dye Alexa Fluor 750, which has the emission peak (brown dashed lines in figures 2.2e and 2.3e) overlapped with the LSPR. Due to maximum enhancement at the peaks, we see similar sharpened profiles for the enhanced emissions (brown shaded area) for both single GNR and GNR dimer, as shown in figures 2.2e and 2.3e respectively. Secondly, for Alexa Fluor 633 dye with the emission maximum at $639\ \mathrm{nm}$ (orange dashed lines in figures 2.2e and 2.3e), we see significant red-shift for the emission peaks, enhanced by the single GNR and by GNR dimer, which can be regard as the enhancement of the emission tail by the longitudinal SPR modes of the nanostructures. Yet, due to other enhancement channels according to the hybridized plasmon modes of the GNR dimer, we

see the maximum peak for GNR dimer is located at $724\ \mathrm{nm}$, which is shorter than the peak of $746\ \mathrm{nm}$ for the single GNR. For the similar reason, we see the other peak with slightly smaller value at the wavelength of $658\ \mathrm{nm}$ for GNR dimer. Finally, for Alexa Fluor 555 with the emission peak at $568\ \mathrm{nm}$, we see from figure 2.2e that, at short distance ($d = 0.75\ \mathrm{nm}$) from single GNR, the emission enhancement at the longer wavelength is suppressed by the emission enhancement corresponding to the high-order modes excited at the shorter wavelength. As the molecule moves away from the tip, the enhancement due to high-order modes decrease very fast, and we see emission tail is lifted by the enhancement caused by the LSPR at longer wavelength. For GNR dimer, we see the longer wavelength enhancement for the emission rise up, which can be attributed to the hybridized modes of GNR dimer.

One-photon excited fluorescence enhancement

Since the plasmonic enhancement of the decay rates of the molecules are highly dependent on the exact positions of the spectra, we will approximate the radiative rate enhancement (ξ_{rad}) and the additional non-radiative rate (K_{nr}) for each dye by taking the average of the enhancement factors over the emission spectra of the dyes.

Expectantly, for single GNR, as the dye molecule gets very close to GNR's tip, the decay rate is dominated by the additional non-radiative rate. Shown in figure 2.2f, we see large non-radiative rates ($\sim 10^4$) for the three dyes for small separation ($d \sim 1\ \mathrm{nm}$). The rates drop rapidly as the separation of the dye from the GNR increases. Specifically, at short distance, we obverse largest $< K_{\mathrm{nr}} >$ for Alexa Fluor 555 (green dotted line), which has the strongest emission overlap with short-wavelength absorption band of the GNR, while at larger distance (e.g. $d > 6\ \mathrm{nm}$), Alexa 750 (brown dotted line), having reddest emission band, exhibits the largest non-radiative rate, due to its strongest spectral overlap with the longitudinal SPR. The radiative rate enhancements ($< \xi_{\mathrm{rad}} >$) for the dyes, however, are mainly correlated with the spectral overlaps between their emission bands and the LSPR. As shown in figure 2.2g, at short distance ($d \sim 1\ \mathrm{nm}$), we see the enhancement factors of 6×10^2, 1×10^2 and 4×10^1 for the radiative rates of Alexa Fluor 750, 633 and 555, respectively. For the dimer, as shown in figure 2.3f, the magnitude of non-radiative rates for the dyes are similar to the case of the single GNR ($\sim 10^4$). And, for the radiative decay rates, we see about one order higher enhancement factors for each dye inside the gap of the dimer (figure 2.3g), compared to the enhancement factors by the single GNR when the dyes are very close to the GNR.

The stronger near-field enhancement by the GNR dimer, together with the stronger radiative enhancement, leads to a larger overall enhancement of the fluorescence of the dye inside the gap of the dimer. As shown in figure 2.3i, for Alexa Fluor 750 dye with emission resonant with the longitudinal SPR, we see a maximum overall fluorescence enhancement factor of about 2.6×10^4 inside the gap of the GNR dimer. For the other two dyes, Alexa Fluor 633 and 555, both having absorption bands and emission bands out of resonance with longitudinal SPR, we get enhancement factors of 1.5×10^3 and 20, excited at the off-resonance wavelengths of $660\ \mathrm{nm}$ and $560\ \mathrm{nm}$, respectively. As a comparison, for single GNR, the over enhancement factor for the three dyes are 10^3, 10^0 and 10^{-2}, respectively, as is depicted in figure 2.2i.

Fluorescence lifetime reduction

A direct consequence of the overall enhancements of the radiative decay rate and non-radiative decay rate of a molecule is the reduction of its fluorescence lifetime. Lifetime shortening is crucial for the single-molecule study of an emitter with very long fluorescence lifetime. Here we find that fluorescence lifetime can be strongly reduced in the vicinity of GNR's tip. As depicted in figures 2.2h and 2.3h, for single GNR and GNR dimer, respectively, we see about four-order reduction for the lifetimes of all the three dyes, as the molecule gets close to the GNR's tip ($\mathrm{d} \sim 1\mathrm{nm}$). For single GNR, the lifetime reduction of the molecule is mainly due to the additional non-radiative decay rates, hence the strong lifetime reduction is only restricted to a very tiny region near the GNR's tip. As can be seen in figure 2.2h, the lifetime reduction factors for the dyes increase rapidly to the magnitude of about 10^{-2} as the molecules move away from the tip by a small distance (at the position: $d \sim 3\ \mathrm{nm}$). For GNR dimer, however, the strong lifetime reduction factor at different position inside the gap do not change significantly. As depicted in figure 2.3h, the reduction factor remains in the range of $10^{-4} \sim 10^{-3}$ for all the dyes in the center of the gap.

Two-photon-excited fluorescence enhancement

Another potential application of gold-nanorod based plasmonic structures is to enhance two-photon-excited fluorescence of a molecule. Unlike the one-photon excited fluorescence, two-photon-excited fluorescence is a nonlinear optical process where the excitation of the molecule is due to the absorption of two identical photons, hence the excitation rate is proportional to the square of the incident light intensity: $k_{\mathrm{exc}}^{(2)} = \sigma^{(2)} I_{\mathrm{exc}}^2$. As a consequence, we would expect higher excitation enhancement for two-photon-excited fluorescence than one-photon counterpart in the near-field hotspots, since the enhancement factor is dependent on the square of the near-field intensity. Additionally, two-photon excitation extends the absorption band into longer wavelength, usually in the infrared range, which can be well overlapped with SPR band of GNR to achieve the maximum enhancement for two-photon-excited fluorescence.

Here, we compare the two-photon-excited fluorescence enhancement by the aforementioned single GNR and GNR dimer. We focus on the two dyes, Alexa Fluor 633 and Alexa Fluor 555, since both have two-photon absorption in the infrared range. In the simulation, the excitation wavelength was set as $770\ \mathrm{nm}$ to ensure best excitation enhancement. The emission spectra and the quantum yields of the dyes under two-photon excitation are considered the same as one-photon excited fluorescence.

Figure 2.5 gives the overall fluorescence enhancements for two dyes under two-photon excitation, by the single GNR and by the GNR dimer. From the plot, we see a maximum enhancement factor of about 10^5 for Alexa 633 molecule (orange circles) by a single GNR, while by GNR dimer, the enhancement factor can be as strong as 10^8 (orange dots). The improvement of the overall enhancement by GNR dimer comes from the strong plasmonic coupling between the two GNRs. This causes stronger enhancement for both the excitation rate and radiative rate of the dye, compared to the single GNR. For Alexa Fluor 555, which has shorter wavelength emission band, we see smaller enhancements by GNR dimer ($\sim 10^7$, green dots) and by single GNR ($\sim 10^4$, green circles), which can be attributed to the stronger quenching effects due to additional non-radiative absorption by the gold.

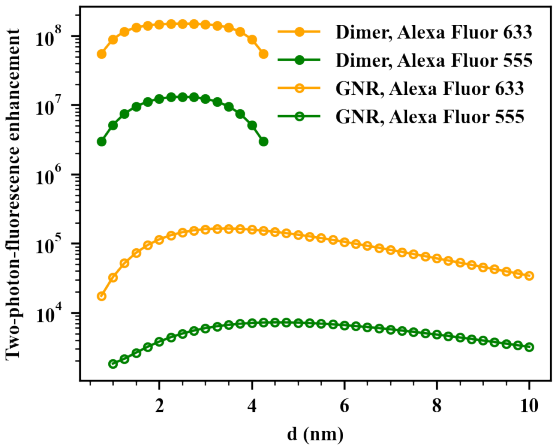

Figure 2.5: Two-photon-excited fluorescence enhancement by a single GNR and by a GNR dimer for two dyes, Alexa Fluor 633 and Alexa Fluor 555.

Saturation of one/two-photon-excited fluorescence enhanced by single GNR or by GNR dimer

In previous discussions, we considered the fluorescence enhancement under very weak excitation, where the processes of excitation and emission can be treated independently. In this case, the emission rate is proportional to the excitation rate of the molecule. As the excitation continue to increase, we will see saturation behavior for the emission rate[4, 30, 39, 40]. For free dye, as the molecule is excited by very high power ($k_{\mathrm{exc}} \to \infty$), from Eq (2.3), we see a limited rate $I^0_{\mathrm{f},\infty} \to k^0_{\mathrm{r}}$ for the emission rate of the free dye, which means the emission rate is limited by the intrinsic radiating rate of the dye (k^0_{r}). Enhanced by the plasmonic structure, the saturated emission rate of the dye is $I_{\mathrm{f},\infty} \to <\xi_{\mathrm{rad}}> \cdot k^0_{\mathrm{r}}$. Therefore, the saturated overall fluorescence enhancement is $<\xi_{\mathrm{rad}}>$, which represents the averaged radiative enhancement of dye by the plasmon structures.

Following the strategy of the book (Principle of Nano-optics) by Novotny and Hecht [4]), the saturation behavior of the molecule can be characterized by the parameter I_{s}. For a free dye, $I_{\mathrm{s}} = k^0_{\mathrm{r}}/\eta_0 = \tau_0^{-1} = k^0_{\mathrm{D}}$, where k^0_{D} and τ_0 are the intrinsic decay rate and intrinsic lifetime of the dye, respectively. For the dye enhanced by a plasmonic structure,

$$I_{\mathrm{s}} = \frac{<\xi_{\mathrm{rad}} + K_{\mathrm{nr}}/k^0_{\mathrm{r}} - 1> \cdot \eta_0 + 1}{\xi_{\mathrm{exc}}} \cdot k^0_{\mathrm{D}}, \tag{2.15}$$

where $< \cdots >$ represents the average over the emission spectrum. Here, I_{s} characterises the saturated excitation power, at which the emission rate equals to half of the saturated emission rate. Obviously, the saturated excitation rate of the molecule, with or without the plasmonic structure, is proportional to the ratio of the total decay rates over the excitation rates.

Next, we investigate the saturation of the fluorescence enhanced by a single GNR and by the GNR dimer. In this study, we represented the enhancements of the decay rates (ξ_{rad} and

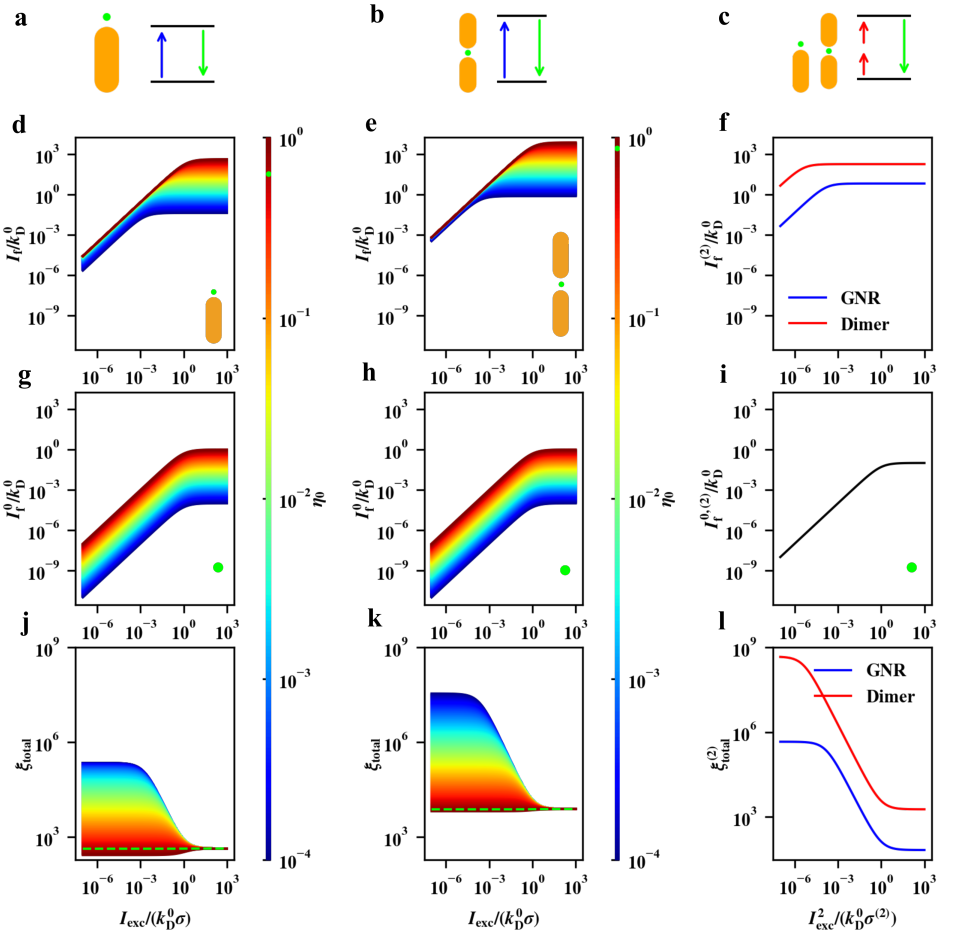

Figure 2.6: Fluorescence saturation under one-photon and two-photon excitation. (a, b, c) Schemes of the simulations for one-photon excited fluorescence enhanced by a single GNR (a) and by a GNR dimer (b), for two-photon-excited fluorescence enhanced by the single GNR and GNR dimer (c). For all cases, the distance from GNR's tip was set as 2.5 nm and the excitation wavelength was set as 765 nm. (d, e, g, h, j, k) Saturation of the one-photon excited fluorescence for single dye molecule with different quantum yields. (d, e, g, h) Excitation power dependence of the one-photon fluorescence with (d, e) or without (e ,h) the enhancement by single GNR (d) or by GNR dimer (e). (j, k) Overall fluorescence enhancement by single GNR (j) or by the GNR dimer (k). Green dashed lines in (j, k) represent the dyes that have constant enhancement factor for all excitation powers by single GNR (j) or by GNR dimer (k), with the quantum yields corresponding to the green dots in the colorbars. Here, for simplicity, we assumed the dyes with different quantum yields have similar one-photon absorption cross section of σ, and their emission spectra were all represented by the emission of Alexa Fluor 750 in the simulations. (f, i, l) Saturation of two-photon-excited fluorescence of a single molecule of Alexa Fluor 633. (f, i) Power dependence of two-photon fluorescence rates with (f) or without (i) the enhancement by single GNR or by GNR dimer. (l) Power dependence of two-photon fluorescence enhancement by single GNR or by GNR dimer.

$K_{\mathrm{nr}}/k_{\mathrm{r}}^0$) with the averaged enhancement factors for a single molecule of Alexa Fluor 750. The molecule was placed at the position of $d = 2.5$ nm from the GNR's tip, or placed at the center of the dimer's gap, as is shown in figures 2.6a, and 2.6b. The excitation enhancement factors were considered as the enhancements of the near-field intensities excited at the wavelength of 770 nm.

We show the fluorescence rate of the molecule as a function of the excitation rate in figures 2.6d, 2.6e, 2.6g, and 2.6h, with (d and e) or without (g and h) the enhancement by single GNR and GNR dimer, respectively. As an assumption, we varied the quantum yield of the molecule from 10^{-4} to 1 to investigate the emission saturation for the dyes with different quantum yield, keeping the intrinsic decay rate ($k_{\mathrm{D}}^0 = 1/\tau_0$) of the dye and the emission spectrum as constant. As expected and shown in the plots, the fluorescence rate depends linearly on the excitation rate for small excitation intensities. At high excitation rate, the emission intensities approach the saturated rates, which could be ether $< \xi_{\mathrm{rad}} > \cdot k_{\mathrm{D}}^0 \cdot \eta_0$ or $k_{\mathrm{D}}^0 \cdot \eta_0$, depending on whether the dye is enhanced or not by the plasmonic structures. Interestingly, from figures 2.6d and 2.6e, we see that the dye with smaller quantum yield is easier to be saturated under the enhancement of the single GNR or the dimer, based on the assumption of similar intrinsic decay rate for all quantum yields.

We compare the overall fluorescence enhancements by the single GNR and by the GNR dimer for the dyes with different quantum yields in figures 2.6j and 2.6k, respectively. For each plasmonic structure, below saturation, the fluorescence enhancement factor does not depend on the excitation power, yet it does depend on the quantum yield of the molecule. It turns out that the overall fluorescence enhancement is larger for the dye with smaller quantum yield. Specifically, the enhancement factor $\xi_{\mathrm{total}} \rightarrow \xi_{\mathrm{exc}} \cdot < \xi_{\mathrm{rad}} >$, as the quantum yield $\eta_0 \rightarrow 0$. Here, ξ_{exc} is the excitation enhancement by the plasmon mode. Above saturation, however, the overall enhancement for all quantum yields approaches to the same enhancement factor of $< \xi_{\mathrm{rad}} >$. By having a closer look at Eq (2.5), we find that for the dye with the quantum yield of

$$\eta_0 = \frac{\xi_{\mathrm{exc}} - 1}{< \xi_{\mathrm{rad}} + K_{\mathrm{nr}}/k_{\mathrm{r}}^0 - 1 >}, \tag{2.16}$$

we see a constant enhancement factor of ξ_{rad} for all excitation powers, which can be confirmed by the straight lines (green dashed) in figure 2.6j and 2.6k.

Finally, it is also of interest to investigate the saturation of two-photon-excited fluorescence, with the enhancement by the single and dimer GNR. As an example, we considered the Alexa Fluor 633 dye excited at the wavelength of 770 nm. Similar to one-photon case, the molecule was placed at the position of $d = 2.5$ nm from the GNR's tip, or placed at the center of the dimer's gap, as shown in figure 2.6c. Due to the stronger excitation enhancement, the fluorescence enhanced by the GNR dimer is saturated at smaller excitation intensity, compared to the single GNR (figure 2.6f). The expected fluorescence rates, excited at high power, are also limited to the saturated emission rates of $< \xi_{\mathrm{rad}} > \cdot k_{\mathrm{D}}^0 \cdot \eta_0$ for both structures. At weak excitation, we see much stronger fluorescence enhancement under two-photon excitation compared to one-photon excitation, which is about 10^8 by the GNR dimer, and 10^5 by the single GNR, as shown in figure 2.6l. The saturated fluorescence enhancement, however, is the same factor of $< \xi_{\mathrm{rad}} >$ for both two-photon excitation and one-photon excitation, which is the averaged enhancement factor of the radiative rate of the dye by the plasmonic structure.

2.4. Conclusions

In conclusion, we theoretically investigated the fluorescence enhancement by a single GNR and by an end-to-end GNR dimer. Compared to single GNR, the GNR dimer with end-to-end configuration provides stronger enhancements for both near-field intensity and radiative rate of a dipole. At low excitation power, the stronger near-field enhancement, together with the stronger radiative enhancement, will introduce much higher overall fluorescence enhancement of a single molecule, especially for the two-photon-excited fluorescence, since two-photon excitation depends quadratically on the excitation intensity. For a GNR dimer with interparticle gap of $5\ \mathrm{nm}$, we got enhancement factor of 10^4 for the dye with well spectral overlapping with the SPR under one photon excitation, which is more than 10 times higher than the enhancement by the single GNR. For two-photon-excited fluorescence, the enhancement can reach up to the factor of 10^8 by GNR dimer, while for single GNR, the maximum enhancement factor is about 10^5. Accompanied with the fluorescence enhancement, we also saw significant spectral shaping and lifetime shortening for the fluorescence of the molecule. Finally, we examined the fluorescence saturation under the enhancement of single GNR and GNR dimer. Theoretical analysis showed that, at very high excitation power, the enhanced fluorescence rate from a single molecule will be saturated to a limited value, which is determined by the intrinsic radiative rate of the molecule, enhanced by the factor of the radiative enhancement by the plasmonic structure.

References

[1] Heinz Raether. Surface plasmons. *Springer Tracts in Modern Physics*, 111:1, 1988.

[2] Uwe Kreibig and Michael Vollmer. *Optical properties of metal clusters*, volume 25. Springer Science & Business Media, 2013.

[3] Craig F Bohren and Donald R Huffman. *Absorption and scattering of light by small particles*. John Wiley & Sons, 2008.

[4] Lukas Novotny and Bert Hecht. *Principles of nano-optics*. Cambridge university press, 2012.

[5] Jon A. Schuller, Edward S. Barnard, Wenshan Cai, Young Chul Jun, Justin S. White, and Mark L. Brongersma. Plasmonics for extreme light concentration and manipulation. *Nature Materials*, 9(3):193–204, March 2010.

[6] Surbhi Lal, Stephan Link, and Naomi J. Halas. Nano-optics from sensing to waveguiding. *Nature Photonics*, 1(11):641–648, November 2007.

[7] Palash Bharadwaj, Pascal Anger, and Lukas Novotny. Nanoplasmonic enhancement of single-molecule fluorescence. *Nanotechnology*, 18(4):044017, December 2006.

[8] Pascal Anger, Palash Bharadwaj, and Lukas Novotny. Enhancement and Quenching of Single-Molecule Fluorescence. *Physical Review Letters*, 96(11):113002, March 2006.

[9] Anika Kinkhabwala, Zongfu Yu, Shanhui Fan, Yuri Avlasevich, Klaus Müllen, and W. E. Moerner. Large single-molecule fluorescence enhancements produced by a bowtie nanoantenna. *Nature Photonics*, 3(11):654–657, November 2009.

[10] S. Sun, L. Wu, P. Bai, and C. E. Png. Fluorescence enhancement in visible light: Dielectric or noble metal? *Physical Chemistry Chemical Physics*, 18(28):19324–19335, July 2016.

[11] Guowei Lu, Tianyue Zhang, Wenqiang Li, Lei Hou, Jie Liu, and Qihuang Gong. Single-Molecule Spontaneous Emission in the Vicinity of an Individual Gold Nanorod. *The Journal of Physical Chemistry C*, 115(32):15822–15828, August 2011.

[12] Haifeng Yuan, Saumyakanti Khatua, Peter Zijlstra, Mustafa Yorulmaz, and Michel Orrit. Thousand-fold Enhancement of Single-Molecule Fluorescence Near a Single Gold Nanorod. *Angewandte Chemie*, 125(4):1255–1259, 2013.

[13] Saumyakanti Khatua, Pedro M. R. Paulo, Haifeng Yuan, Ankur Gupta, Peter Zijlstra, and Michel Orrit. Resonant Plasmonic Enhancement of Single-Molecule Fluorescence by Individual Gold Nanorods. *ACS Nano*, 8(5):4440–4449, May 2014.

[14] Anastasiya Puchkova, Carolin Vietz, Enrico Pibiri, Bettina Wünsch, María Sanz Paz, Guillermo P. Acuna, and Philip Tinnefeld. DNA Origami Nanoantennas with over 5000-fold Fluorescence Enhancement and Single-Molecule Detection at 25 μM. *Nano Letters*, 15(12):8354–8359, December 2015.

[15] Deep Punj, Raju Regmi, Alexis Devilez, Robin Plauchu, Satish Babu Moparthi, Brian Stout, Nicolas Bonod, Hervé Rigneault, and Jérôme Wenger. Self-Assembled Nanoparticle Dimer Antennas for Plasmonic-Enhanced Single-Molecule Fluorescence Detection at Micromolar Concentrations. *ACS Photonics*, 2(8):1099–1107, August 2015.

[16] Biswajit Pradhan, Saumyakanti Khatua, Ankur Gupta, Thijs Aartsma, Gerard Canters, and Michel Orrit. Gold-Nanorod-Enhanced Fluorescence Correlation Spectroscopy of Fluorophores with High Quantum Yield in Lipid Bilayers. *The Journal of Physical Chemistry C*, 120(45):25996–26003, November 2016.

[17] Weichun Zhang, Martín Caldarola, Xuxing Lu, Biswajit Pradhan, and Michel Orrit. Single-molecule fluorescence enhancement of a near-infrared dye by gold nanorods using DNA transient binding. *Physical Chemistry Chemical Physics*, 20(31):20468–20475, 2018.

[18] Pedro M. R. Paulo, David Botequim, Agnieszka Jóskowiak, Sofia Martins, Duarte M. F. Prazeres, Peter Zijlstra, and Sílvia M. B. Costa. Enhanced Fluorescence of a Dye on DNA-Assembled Gold Nanodimers Discriminated by Lifetime Correlation Spectroscopy. *The Journal of Physical Chemistry C*, 122(20):10971–10980, May 2018.

[19] Xuxing Lu, Gang Ye, Deep Punj, Ryan C. Chiechi, and Michel Orrit. Quantum Yield Limits for the Detection of Single-Molecule Fluorescence Enhancement by a Gold Nanorod. *ACS Photonics*, 7(9):2498–2505, September 2020.

[20] E. M. Purcell, H. C. Torrey, and R. V. Pound. Resonance Absorption by Nuclear Magnetic Moments in a Solid. *Physical Review*, 69(1-2):37–38, January 1946.

[21] Daniel Kleppner. Inhibited Spontaneous Emission. *Physical Review Letters*, 47(4):233–236, July 1981.

[22] W. L. Barnes. Fluorescence near interfaces: The role of photonic mode density. *Journal of Modern Optics*, 45(4):661–699, April 1998.

[23] Joseph R Lakowicz. *Principles of fluorescence spectroscopy*. Springer science & business media, 2013.

[24] Alexander Huck, Shailesh Kumar, Abdul Shakoor, and Ulrik L. Andersen. Controlled Coupling of a Single Nitrogen-Vacancy Center to a Silver Nanowire. *Physical Review Letters*, 106(9):096801, February 2011.

[25] Ling Xin, Mo Lu, Steffen Both, Markus Pfeiffer, Maximilian J. Urban, Chao Zhou, Hao Yan, Thomas Weiss, Na Liu, and Klas Lindfors. Watching a Single Fluorophore Molecule Walk into a Plasmonic Hotspot. *ACS Photonics*, 6(4):985–993, April 2019.

[26] M. Ringler, A. Schwemer, M. Wunderlich, A. Nichtl, K. Kürzinger, T. A. Klar, and J. Feldmann. Shaping Emission Spectra of Fluorescent Molecules with Single Plasmonic Nanoresonators. *Physical Review Letters*, 100(20):203002, May 2008.

[27] G. Vecchi, V. Giannini, and J. Gómez Rivas. Shaping the Fluorescent Emission by Lattice Resonances in Plasmonic Crystals of Nanoantennas. *Physical Review Letters*, 102(14):146807, April 2009.

[28] Marcus Schmelzeisen, Yi Zhao, Markus Klapper, Klaus Müllen, and Maximilian Kreiter. Fluorescence Enhancement from Individual Plasmonic Gap Resonances. *ACS Nano*, 4(6):3309–3317, June 2010.

[29] Oluwafemi S. Ojambati, Rohit Chikkaraddy, William M. Deacon, Junyang Huang, Demelza Wright, and Jeremy J. Baumberg. Efficient Generation of Two-Photon Excited Phosphorescence from Molecules in Plasmonic Nanocavities. *Nano Letters*, 20(6):4653–4658, June 2020.

[30] Martin Kauert, Patrick C. Stoller, Martin Frenz, and Jaro Rička. Absolute measurement of molecular two-photon absorption cross-sections using a fluorescence saturation technique. *Optics Express*, 14(18):8434–8447, September 2006.

[31] Mark W. Dowley, Kenneth B. Eisenthal, and Warner L. Peticolas. Two-Photon Laser Excitation of Polycyclic Aromatic Molecules. *The Journal of Chemical Physics*, 47(5):1609–1619, September 1967.

[32] Mariacristina Rumi and Joseph W. Perry. Two-photon absorption: An overview of measurements and principles. *Advances in Optics and Photonics*, 2(4):451–518, December 2010.

[33] M. T. Homer Reid and S. G. Johnson. Efficient Computation of Power, Force, and Torque in BEM Scattering Calculations. *ArXiv e-prints*, July 2013.

[34] `http://github.com/homerreid/scuff-EM`.

[35] Taishi Zhang, Nengyue Gao, Shuang Li, Matthew J. Lang, and Qing-Hua Xu. Single-Particle Spectroscopic Study on Fluorescence Enhancement by Plasmon Coupled Gold Nanorod Dimers Assembled on DNA Origami. *The Journal of Physical Chemistry Letters*, 6(11):2043–2049, June 2015.

[36] András Szenes, Balázs Bánhelyi, Tibor Csendes, Gábor Szabó, and Mária Csete. Enhancing Diamond Fluorescence via Optimized Nanorod Dimer Configurations. *Plasmonics*, 13(6):1977–1985, December 2018.

[37] Manshu Peng, Feifei Sun, Na Na, and Jin Ouyang. Target-Triggered Assembly of Nanogap Antennas to Enhance the Fluorescence of Single Molecules and Their Application in MicroRNA Detection. *Small*, 16(19):2000460, 2020.

[38] Zhi Zhao, Xiahui Chen, Jiawei Zuo, Ali Basiri, Shinhyuk Choi, Yu Yao, Yan Liu, and Chao Wang. Deterministic assembly of single emitters in sub-5 nanometer optical cavity formed by gold nanorod dimers on three-dimensional DNA origami. *Nano Research*, August 2021.

[39] John W. Daily. Saturation effects in laser induced fluorescence spectroscopy. *Applied Optics*, 16(3):568–571, March 1977.

[40] Keith Berland and Guoqing Shen. Excitation saturation in two-photon fluorescence correlation spectroscopy. *Applied Optics*, 42(27):5566–5576, September 2003.